JOURNAL OF AIRCRAFT
Vol. 38, No. 6, November–December 2001

Maneuver Trim Optimization Techniques for Active Aeroelastic Wings

P. Scott Zink,* Dimitri N. Mavris,† and Daniella E. Raveh‡
Georgia Institute of Technology, Atlanta, Georgia 30332-0150

A method for performing trim optimization of active aeroelastic wing (AAW) technology, based on posing the trim problem as a linear programming problem and solving it with the simplex method, is presented. Trim optimization is then integrated with the structural design process in a sequential manner, such that new optimal deflections of the control surfaces are computed for every structural design iteration. The use of the simplex method for trim optimization allowed the elimination of nonphysical constraints that had to be imposed when a gradient-based method was used. This resulted in significantly better objectives for the trim optimization. The sequential AAW design process was demonstrated on a lightweight fighter-type aircraft performing symmetric and antisymmetric maneuvers at subsonic and supersonic speeds. The concurrent trim and structural optimization resulted in a significantly lighter structure compared to a structure designed with conventional control technology and to a structure employing AAW technology with fixed control-surface deflections.

Introduction

AN EMERGING and promising technology for addressing the problem of adverse aeroelastic deformation, such as control-surface reversal, is active aeroelastic wing (AAW) technology. It has recently been a key area of study for both the government and industry[1,2] and is defined by Pendleton et al. as "a multidisciplinary, synergistic technology that integrates air vehicle aerodynamics, active controls, and structures together to maximize air vehicle performance."[3] AAW technology exploits the use of leading- and trailing-edge control surfaces to aeroelastically shape the wing, with the resulting aerodynamic forces from the flexible wing becoming the primary means for generating control power. With AAW the control surfaces then act mainly as tabs and not as the primary sources of control power as they do with a conventional control philosophy. As a result, wing flexibility is seen as an advantage rather than a detriment because the aircraft can be operated beyond reversal speeds and still generate the required control power for maneuvers. Hence, there is potential for significant reductions in structural weight and actuator power.

Figure 1 illustrates conceptually the differences between AAW technology and a conventional control approach. The hypothetical example shows the cross section of two wings deforming as a result of aeroelastic effects. The upper wing, employing AAW technology, is twisting in a positive way with the use of both leading- and trailing-edge surfaces, whereas the conventionally controlled, lower wing, which uses only the trailing-edge surface, is twisting in a negative way.[4] This adverse twist caused by the deflection of the trailing-edge surface is associated with reduced control surface effectiveness and control-surface reversal, in which the increase in camber caused by the deflection of the surface is offset by the negative twist of the wing.

Because AAW technology is multidisciplinary in nature, structural design using the technology necessarily requires detailed information about the vehicle structures, aerodynamics, and controls, and in particular, is heavily dependent on control law design, which in turn depends on the flexible structure. As a result, there is a need for an AAW design process in which the structure and control laws are optimized concurrently.

In consideration of AAW technology's use of redundant control surfaces, important constituents of the technology are control surface gear ratios, which dictate how one control surface deflects with respect to a single basis surface. Two gear ratio scenarios are illustrated in Fig. 2, in which the deflections of the leading-edge inboard (LEI), leading-edge outboard (LEO), and trailing-edge inboard (TEI) surfaces are linearly dependent on the deflection of the trailing-edge outboard surface (TEO). The gear ratios significantly influence the aeroelastic load distribution and, hence, affect internal loads and structural deformation. For the purposes of this research, the gear ratios constitute the control laws.

The AAW design process refers to the concurrent optimization of the structure and the gear ratios. Structural optimization refers to the sizing of structural elements (e.g., skin thickness, spar thickness) to minimum weight, subject to stress, aeroelastic constraints, etc. Optimization of the gear ratios, more commonly known as trim optimization, is the process of selecting the gear ratios, or control-surface deflection angles, that trim the aircraft to a prescribed maneuver while minimizing some objective function. The need for trim optimization is caused by AAW technology's use of redundant control surfaces, which means that the static aeroelastic trim equations cannot be solved in a closed-form manner.

Volk and Ausman[5] added a trim optimization capability to ASTROS,[6] a finite element-based structural optimization code. The trim optimization objective was to minimize the overall control-surface actuator command signal or, in other terms, control energy. The optimization was performed by using a Newton–Raphson method. A latter version of the program incorporated the ability to also limit the control-surface hinge moments.[7] Applications of these trim optimization capabilities in ASTROS can be found in Refs. 8 and 9 in which control-surface gearing was studied for rolling maneuvers of a fighter-type aircraft using AAW technology. Similarly, Miller[10] formulated the trim optimization problem as a minimization of a control-surface energy function, subject to bending moments, torsion, hinge moments, roll rate, and roll acceleration constraints. The process employed a gradient-based optimization algorithm. As an evolution of Miller's work, Zillmer[11] posed trim optimization as the minimization of a composite function of stress, induced drag, and buckling load. Trim optimization was performed in the Integrated Structure/Maneuver Design (ISMD) program. Stability derivatives that are necessary for trim balance, and sensitivities of the objectives with respect to the control-surface deflections, were obtained from a NASTRAN[12] static aeroelastic analysis.

Received 30 June 2000; revision received 6 December 2000; accepted for publication 12 January 2001.

*Ph.D. Candidate, School of Aerospace Engineering. Student Member AIAA.
†Boeing Chair in Advanced Aerospace Systems Analysis, School of Aerospace Engineering. Associate Fellow AIAA.
‡Research Engineer II, School of Aerospace Engineering. Member AIAA.

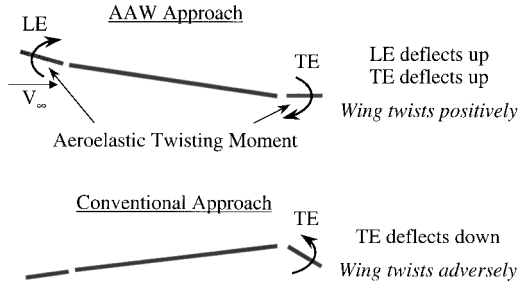

Fig. 1 AAW technology vs conventional control.

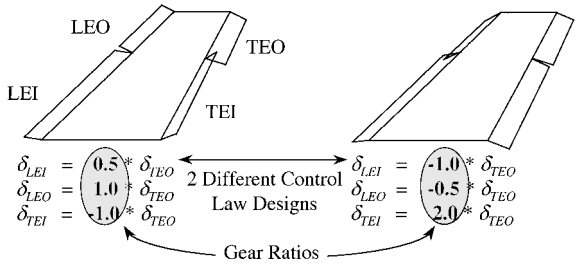

Fig. 2 Gear ratio illustration.

Zillmer[11] and Dobbs et al.[13] developed an iterative approach to the AAW design process, in which the trim optimization algorithm implemented in ISMD, just discussed, is embedded in an iterative process with NASTRAN. The maneuver loads caused by the optimized deflections from ISMD are transferred to NASTRAN, which then optimizes the structure to minimum weight. NASTRAN then passes stability derivative and sensitivity information of the current structural design to ISMD for another trim optimization. This process repeats itself until the wing weight converges.

Love et al.[14] proposed a generalized trim capability in which any linear combination of component loads (section bending moment, torsion, hinge moments, etc.), or trim parameters, could be the objective of the trim optimization problem. In addition, component loads could be considered as constraints. The optimization problem was solved by a modified method of feasible directions algorithm (MMOFD),[15] which is the optimization algorithm implemented in ASTROS for structural optimization. However, the MMOFD is not the ideal algorithm for solving the trim optimization problem (as will be discussed in more detail in a following section), and this led to the necessity of imposing additional constraints on the problem. The method was implemented in ASTROS so that stability derivatives and sensitivity information were not obtained from an external source. Zink et al.[16] applied the techniques of Ref. 14 in a design study of a generic lightweight fighter concept employing AAW technology. Trim optimization was performed for symmetric (pull-up, push-over) and antisymmetric (rolling) maneuvers. The intention was that trim and structural optimization would be repeated iteratively as proposed in Ref. 14. However, only the first step was demonstrated, as trim optimization was performed only once on the starting structural design.

The difficulties with trim optimization in Ref. 16 have prompted the authors to explore other means of solving the trim optimization problem. Recognizing that both the symmetric and antisymmetric trim problems are linear, the authors propose that the optimization problem can be posed as a linear programming (LP) problem and solved by the simplex method.[17–19] Then, the optimal control-surface deflections, resulting from trim optimization, are converted to gear ratios and used in a structural optimization within ASTROS. Following the proposed process of Ref. 14, a sequential design process is demonstrated that iterates between trim optimization and structural optimization steps, until the optimal structure with its optimal control-surface deflections are obtained. The paper presents a comparison between results of trim optimization performed with the MMOFD and the simplex algorithms. An AAW design study is performed on a lightweight composite fighter aircraft. The optimal structural design obtained by the sequential AAW design process is then compared to the structural design of an AAW whose control law remains fixed over the course of the structural optimization. In addition, comparison is made to a conventionally controlled wing, indicating some of the weight benefits associated with the use of AAW technology.

Methodology

Static Aeroelastic Equation

The basic equation for the static aeroelastic analysis of a free aircraft by the finite element method in discrete coordinates is[20]

$$[[K] - q[AICS]]\{u\} + [M][\phi_r]\{\ddot{u}_r\} = [P]\{\delta\} \tag{1}$$

where $[K]$ is the stiffness matrix, $[AICS]$ is the aerodynamic influence coefficients matrix transformed to the structural degrees of freedom, $\{u\}$ are the displacements and rotations at the structural nodes, $[M]$ is the mass matrix, $[\phi_r]$ are the rigid-body modes of the free aircraft, $\{\ddot{u}_r\}$ is a vector of rigid-body accelerations, $[P]$ is a matrix of the rigid aerodynamic force coefficients caused by aerodynamic trim parameters, q is the dynamic pressure, and $\{\delta\}$ is the vector of aerodynamic trim parameters (e.g., angle of attack, aileron deflection, steady roll rate). For a free aircraft Eq. (1) is solved together with the following constraint on the elastic displacements[21]:

$$[\phi_r]^T[M]\{u\} = \{0\} \tag{2}$$

Substitution of $\{u\}$ from Eq. (1) into Eq. (2) yields the trim equation[20]:

$$[L]\{\ddot{u}_r\} = [R]\{\delta\} \tag{3}$$

where $[L]$ is the resultant aeroelastic mass and $[R]$ is the resultant aeroelastic trim forces. In the case where the number of free trim parameters $\{\delta\}$ is equal to the number of rigid-body modes $\{\ddot{u}_r\}$, Eq. (3) has a closed-form solution. However, if multiple control surfaces (i.e., redundant surfaces) are desired to trim the aircraft, then the closed-form solution no longer exists. The trim solution must then be formulated as an optimization problem (i.e., trim optimization) to determine the combination of control-surface deflections that trim the aircraft and minimize an objective of interest to the structural designer.

Trim Optimization by MMOFD

Trim optimization by the MMOFD is performed for both symmetric and antisymmetric maneuvers. For the symmetric maneuvers the trim optimization problem is posed as a minimization of root bending moment (RBM), where the wing control surfaces are used to tailor the load distribution and provide load relief at the wing root, thus ultimately reducing wing weight.

The symmetric trim optimization problem[16] is formally stated as

Minimize:

$$\text{RBM} = \sum_{i=1}^{n_{cs}} \left[\frac{\partial(\text{RBM})}{\partial \delta_i}\right]_{\text{flex}} \delta_i + \left[\frac{\partial(\text{RBM})}{\partial \alpha}\right]_{\text{flex}} \alpha \tag{4}$$

Subject to:

Control-surface travel limits:

$$-30 \text{ deg} \le \delta_{\text{LEI}} \le 5 \text{ deg}, \qquad -30 \text{ deg} \le \delta_{\text{LEO}} \le 5 \text{ deg}$$

$$-30 \text{ deg} \le \delta_{\text{TEI}} \le 30 \text{ deg}, \qquad -30 \text{ deg} \le \delta_{\text{TEO}} \le 30 \text{ deg}$$

$$-30 \text{ deg} \le \delta_{\text{HT}} \le 30 \text{ deg}, \qquad -10 \text{ deg} \le \alpha \le 30 \text{ deg}$$

Hinge moment (HM) constraints:

$$-3.0 \times 10^5 \le \text{HM}_{\text{LEI}} \le 3.0 \times 10^5$$

$$-1.0 \times 10^5 \le \text{HM}_{\text{LEO}} \le 1.0 \times 10^5$$

$$-1.5 \times 10^5 \le \text{HM}_{\text{TEI}} \le 1.5 \times 10^5$$

$$-5.0 \times 10^4 \le \text{HM}_{\text{TEO}} \le 5.0 \times 10^4 \text{ lb-in.}$$

where the HM for each control surface (cs) is given by

$$\mathrm{HM_{cs}} = \sum_{i=1}^{n_{cs}} \left[\frac{\partial(\mathrm{HM_{cs}})}{\partial \delta_i}\right]_{\mathrm{flex}} \delta_i + \left[\frac{\partial(\mathrm{HM_{cs}})}{\partial \alpha}\right]_{\mathrm{flex}} \alpha + \left[\frac{\partial(\mathrm{HM_{cs}})}{\partial a_z}\right]_{\mathrm{flex}} a_z \tag{5}$$

Satisfaction of trim equations (lift and pitching moment balance):

$$\sum_{i=1}^{n_{cs}} \left(\frac{\partial L}{\partial \delta_i}\right)_{\mathrm{flex}} \delta_i + \left(\frac{\partial L}{\partial \alpha}\right)_{\mathrm{flex}} \alpha + L_{\mathrm{const}} = m a_z \tag{6}$$

$$\sum_{i=1}^{n_{cs}} \left(\frac{\partial M}{\partial \delta_i}\right)_{\mathrm{flex}} \delta_i + \left(\frac{\partial M}{\partial \alpha}\right)_{\mathrm{flex}} \alpha + M_{\mathrm{const}} = 0 \tag{7}$$

The design variables are α, δ_{LEI}, δ_{LEO}, δ_{TEI}, δ_{TEO}, and δ_{HT}, where HT is the horizontal tail, α is the angle of attack, δ_i are the control-surface deflections, a_z is the vertical acceleration, m is the aircraft mass, n_{cs} is the number of control surfaces, and L_{const} and M_{const} refer to the lift and moment terms that are not dependent on control-surface deflection and angle of attack. The lift and moment derivatives of Eqs. (6) and (7) are the dimensional flexible stability derivatives, estimated from the trim equation (3). Similarly, the flexible component load derivatives $[\partial(\mathrm{RBM})/\partial\delta, \partial(\mathrm{HM})/\partial\delta]$ are estimated by multiplying the applied loads (both inertial and aeroelastic) caused by a unit deflection of the trim parameter, by an appropriate matrix that represents the moment arm from each grid point to the section about which the moment is being calculated. The control-surface travel limits and hinge moment limits are based on typical allowables for modern fighter aircraft. The effect of pitch rate is assumed to be negligible.

For the antisymmetric maneuvers trim optimization is formulated as a minimization of the total hinge moments, subject to the surface travel limits, hinge moment constraints, and trim balance requirements, as given formally by

Minimize:

$$\mathrm{HM_{LEI}} + \mathrm{HM_{LEO}} + \mathrm{HM_{TEI}} + \mathrm{HM_{TEO}}$$

Subject to:

Control-surface travel limits:

$$-30 \text{ deg} \le \delta_{\mathrm{LEI}} \le 5 \text{ deg}, \qquad -30 \text{ deg} \le \delta_{\mathrm{LEO}} \le 5 \text{ deg}$$

$$-30 \text{ deg} \le \delta_{\mathrm{TEI}} \le 30 \text{ deg}, \qquad -30 \text{ deg} \le \delta_{\mathrm{TEO}} \le 30 \text{ deg}$$

HM constraints:

$$-3.0 \times 10^5 \le \mathrm{HM_{LEI}} \le 3.0 \times 10^5$$

$$-1.0 \times 10^5 \le \mathrm{HM_{LEO}} \le 1.0 \times 10^5$$

$$-1.5 \times 10^5 \le \mathrm{HM_{TEI}} \le 1.5 \times 10^5$$

$$-5.0 \times 10^4 \le \mathrm{HM_{TEO}} \le 5.0 \times 10^4 \text{ lb-in.}$$

where the HM for each control surface is

$$\mathrm{HM_{cs}} = \sum_{i=1}^{n_{cs}} \left[\frac{\partial(\mathrm{HM_{cs}})}{\partial \delta_i}\right]_{\mathrm{flex}} \delta_i + \left[\frac{\partial(\mathrm{HM_{cs}})}{\partial p}\right]_{\mathrm{flex}} p \tag{8}$$

Satisfaction of trim equations (roll moment balance):

$$\sum_{i=1}^{n_{cs}} \left(\frac{\partial \ell}{\partial \delta_i}\right)_{\mathrm{flex}} \delta_i + \left(\frac{\partial \ell}{\partial p}\right)_{\mathrm{flex}} p = 0 \tag{9}$$

The design variables are δ_{LEI}, δ_{LEO}, δ_{TEI}, δ_{TEO}, where ℓ is rolling moment and p is the user-specified roll rate. The minimization of hinge moments turned out to be difficult, as initially the optimizer would drive the hinge moments to large negative values, which were as bad as large positive values. This is because positive (downward) deflection of the trailing-edge surfaces produces negative hinge moment. To prevent this, for the subsonic rolling maneuver, $\mathrm{HM_{TEI}}$ and $\mathrm{HM_{TEO}}$ were constrained to be negative and multiplied by negative one in the objective. For the supersonic rolling maneuver the trailing-edge hinge moments were constrained to be positive because the trailing-edge surfaces were found to be reversing. These difficulties prompted the authors to explore more suitable methods for performing the trim optimization. The next section poses trim optimization as a LP problem to be solved by the simplex method.

Trim Optimization by the Simplex Method

The simplex method[19] is a non-gradient-based algorithm, designed for the solution of LP problems. A LP problem is an optimization problem whose objective and constraints (inequality and/or equality) are linear functions of the design variables. One of the features of the simplex method is that typically, for well-posed problems, the algorithm converges to the exact optimal solution.

The symmetric trim optimization problem, as formulated in the preceding section, is already cast in the form of a LP problem. The antisymmetric problem, as it is posed, is also a LP problem. However, to overcome the difficulties of the MMOFD algorithm driving the hinge moments to large negative values, the antisymmetric trim problem is cast as a minimization of a function, which is defined as the summation of the absolute value of each hinge moment term. Mathematically, the new objective function for the antisymmetric maneuvers is written as

Minimize:

$$|\mathrm{HM_{LEI}}| + |\mathrm{HM_{LEO}}| + |\mathrm{HM_{TEI}}| + |\mathrm{HM_{TEO}}| \tag{10}$$

where each hinge moment term ($\mathrm{HM_{LEI}}$, $\mathrm{HM_{LEO}}$, etc.) is again defined by Eq. (8) and is a linear function of the trim parameter design variables (δ_{LEI}, δ_{LEO}, etc.). As a result of taking the absolute value of each hinge moment, the inherent linearity of the original objective function with respect to the design variables is eliminated, and thus the minimization of Eq. (10) does not constitute a LP problem. However, it can be equivalently posed as a LP problem by defining a new minimization problem in which each hinge moment term of the objective $|\mathrm{HM_{cs}}|$ is replaced with a new design variable e_{cs}, which is constrained to be greater than or equal to the absolute value of the hinge moment. This formulation results in two additional constraints for each term,[17] and the minimization of Eq. (10) is then posed as

Minimize:

$$e_{\mathrm{LEI}} + e_{\mathrm{LEO}} + e_{\mathrm{TEI}} + e_{\mathrm{TEO}}$$

Subject to:

$$\mathrm{HM_{LEI}} \le e_{\mathrm{LEI}}, \qquad -\mathrm{HM_{LEI}} \le e_{\mathrm{LEI}}, \qquad \mathrm{HM_{LEO}} \le e_{\mathrm{LEO}}$$

$$-\mathrm{HM_{LEO}} \le e_{\mathrm{LEO}}, \qquad \mathrm{HM_{TEI}} \le e_{\mathrm{TEI}}, \qquad -\mathrm{HM_{TEI}} \le e_{\mathrm{TEI}}$$

$$\mathrm{HM_{TEO}} \le e_{\mathrm{TEO}}, \qquad -\mathrm{HM_{TEO}} \le e_{\mathrm{TEO}}$$

The design variables are δ_{LEI}, δ_{LEO}, δ_{TEI}, δ_{TEO}, e_{LEI}, e_{LEO}, e_{TEI}, and e_{TEO}.

The addition of the control-surface travel limits, hinge moment constraints, and the roll balance constraint of Eq. (9) to the preceding LP problem results in the new antisymmetric trim optimization problem in which the summation of the absolute value of the hinge moments is being minimized. The nonphysical constraints that were added when using the MMOFD algorithm, in order to prevent the optimizer from driving the design to large negative values, are now eliminated.

Sequential AAW Design

The sequential AAW design process is performed by iterating between trim optimization, by the simplex method in MATLAB®,[22] and structural optimization by ASTROS, as presented in Fig. 3. For

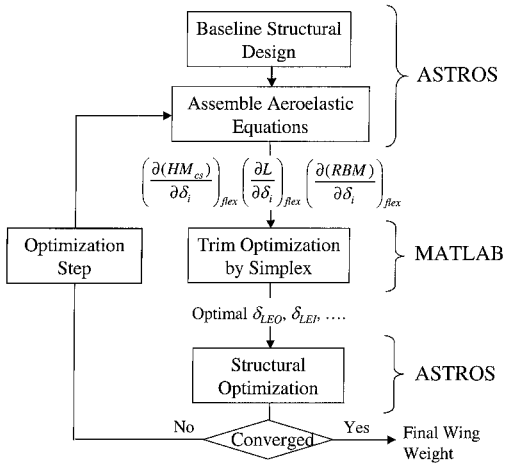

Fig. 3 Sequential AAW design process.

each structural optimization iteration, the control surface deflections for the current structural design are optimized. Then, these new control-surface deflections are converted to gear ratios [eliminating the redundancies of Eq. (3)] and passed to the structural optimizer, which then proceeds to take another step. After the structural optimization step the aeroelastic equations for the new structural design are assembled, and the appropriate stability derivatives, trim objective, and constraint coefficients [needed in Eqs. (4–9)] are calculated in ASTROS and then output to trim optimization. This process repeats itself until the structural optimization objective, wing weight, is converged.

Results

Structural and Aerodynamic Models

The structural model of the aircraft used both in this research and in Ref. 16 is shown in Fig. 4. It is an ASTROS preliminary design finite element model of a lightweight composite fighter aircraft with four wing control surfaces (two trailing edge, two leading edge) and a horizontal tail.[23,24] It corresponds to a wing with an aspect ratio of 3.0, a total planform area of 330 ft^2, a taper ratio of 20%, a leading-edge sweep of 38.7 deg, and a thickness ratio of 3%. The skin of the wing is made up of four composite plies with orientations of 0, ± 45, and 90 deg, where the thickness of the -45 and $+45$-deg plies are constrained to be equal. The composite wing skin plies are designed (tailored) in thickness, via ASTROS optimization routines, to meet specified maneuver and strength requirements.

The aerodynamic model is shown in Fig. 5. It is a flat-panel Carmichael[25] model containing 143 vertical panels and 255 horizontal panels. It also contains paneling for the four wing control surfaces and horizontal tail to coincide with the control surfaces on the structural model. Carmichael aerodynamic influence coefficients are produced for two Mach numbers, 0.95 and 1.2, for both symmetric and antisymmetric conditions.[26]

The design variables for structural optimization are the layer thickness of the composite skins. The number of design variables is 78 as a result of physical linking of the skin elements. Internal structure and carry-through structure remain fixed. Table 1 shows the symmetric and antisymmetric maneuver conditions and strength constraints to which the structure is designed. Whereas a realistic fighter design requires the consideration of asymmetric 3-degree-of-freedom rolling pull-out maneuvers, this study is limited to pure symmetric and antisymmetric maneuvers for simplicity. To account for this, the strength constraints of the antisymmetric maneuvers were lowered, acknowledging that additional strain would result from the symmetric component of the asymmetric maneuver.

Comparison of Simplex Method and MMOFD

For comparison of the MMOFD and simplex algorithms, trim optimization is performed for maneuver 1 (subsonic, symmetric 9-g pull-up), maneuver 3 (supersonic roll), and maneuver 4 (subsonic roll). Trim optimization results for the MMOFD are obtained from Ref. 16. Maneuver 2 is omitted from the comparison as trim optimization by the MMOFD for this maneuver was not performed in Ref. 16. Table 2 shows a comparison of the final results of the two methods for the subsonic rolling maneuver. For trim optimization by the MMOFD, the leading-edge surface deflections were fixed to zero, and the hinge moments for each of the leading-edge surfaces were not considered in the objective. As a result, to compare the MMOFD and the simplex method fairly, trim optimization by the simplex method was first posed to reflect the formulation of the MMOFD. The results of this are in the second column, with the simplex method results matching closely the results of the MMOFD. Trim optimization by the simplex method was then performed without the restriction on the leading-edge surfaces and hinge moments. The results of this optimization are shown in the third column of Table 2, showing that the removal of these restrictions results in a significantly lower total hinge moment.

Table 3 shows a comparison of the MMOFD and the simplex method for the solution of the supersonic antisymmetric trim

Table 1 Maneuver conditions and design constraints

Maneuver condition	Design constraint
1) Mach 0.95, 10,000 ft 9-g pull-up	Fiber strain 3000 $\mu\varepsilon$ tension 2800 $\mu\varepsilon$ compression
2) Mach 1.20, sea level -3-g push-over	Fiber strain 3000 $\mu\varepsilon$ tension 2800 $\mu\varepsilon$ compression
3) Mach 1.20, sea level Steady-state roll = 100 deg/s	Fiber strain 1000 $\mu\varepsilon$ tension 900 $\mu\varepsilon$ compression
4) Mach 0.95, 10,000 ft Steady-state roll = 180 deg/s	Fiber strain 1000 $\mu\varepsilon$ tension 900 $\mu\varepsilon$ compression

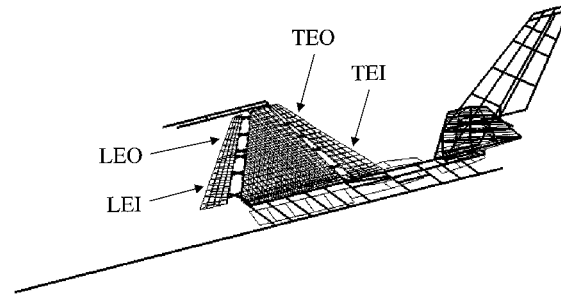

Fig. 4 Structural model of generic fighter.

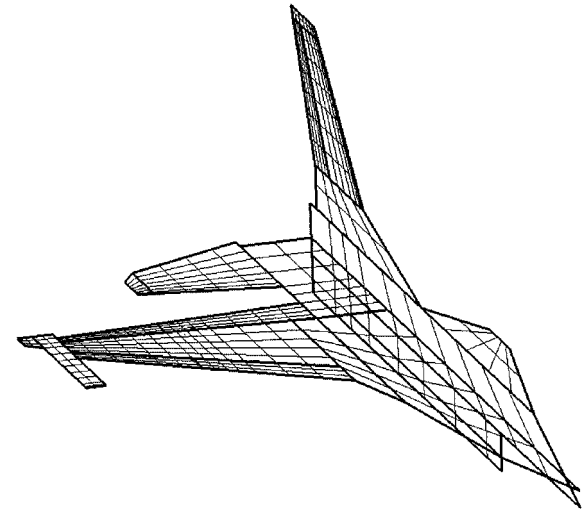

Fig. 5 Aerodynamic model of generic fighter.

Table 2 Trim optimization comparison for subsonic roll

Variable	MMOFD	Simplex (like MMOFD)	Simplex
δ_{LEI}	0.000 deg	0.000 deg	2.565 deg
δ_{LEO}	0.000 deg	0.000 deg	5.000 deg
δ_{TEI}	−1.157 deg	−1.155 deg	−0.960 deg
δ_{TEO}	9.457 deg	9.442 deg	8.854 deg
HM_{LEI}, lb-in.	−25,566.0	−25,560.0	0.000
HM_{LEO}, lb-in.	−23,394.0	−23,389.0	−4,720.0
HM_{TEI}, lb-in.	−0.169	0.000	0.000
HM_{TEO}, lb-in.	−13,325.8	−13,204.4	−12,200.0
Total objective	62,286.0	62,153.0	16,920.0

Table 3 Trim optimization comparison for supersonic roll

Variable	MMOFD	Simplex (like MMOFD)	Simplex
δ_{LEI}	2.792 deg	2.792 deg	0.773 deg
δ_{LEO}	5.000 deg	5.000 deg	2.780 deg
δ_{TEI}	0.255 deg	0.414 deg	0.245 deg
δ_{TEO}	1.605 deg	1.603 deg	13.220 deg
HM_{LEI}, lb-in.	82,610.0	82,600.0	0.000
HM_{LEO}, lb-in.	85,280.0	85,265.0	13,870.0
HM_{TEI}, lb-in.	866.0	0.000	0.000
HM_{TEO}, lb-in.	0.150	0.000	−50,000.0
Total objective	168,756.2	165,200.0	63,870.0

Table 4 Trim optimization comparison for subsonic pull-up

Variable	MMOFD	Simplex
δ_{LEI}	−16.800 deg	−10.599 deg
δ_{LEO}	−30.000 deg	−30.000 deg
δ_{TEI}	−2.140 deg	0.463 deg
δ_{TEO}	−30.000 deg	−30.000 deg
δ_{HT}	1.902 deg	2.698 deg
α	13.032 deg	12.659 deg
HM_{LEI}, lb-in.	252,230.0	300,000.0
HM_{LEO}, lb-in.	100,430.0	100,000.0
HM_{TEI}, lb-in.	8,020.0	−1,480.0
HM_{TEO}, lb-in.	40,380.0	39,920.0
RBM, lb-in.	4,372,700.0	4,351,100.0

problem. In the case of the MMOFD, the trailing-edge hinge moments were constrained to be positive, and once again, in the interest of fairness, an optimization by the simplex method was performed to reflect the formulation of the MMOFD. Both methods produce comparable results, with the simplex converging to a slightly lower total hinge moment. However, without the restriction on the trailing-edge hinge moments being positive, the simplex method uses more of the TEO surface, resulting in a significantly lower objective (column 3).

The results of the trim optimization for the subsonic, symmetric maneuver are shown in Table 4. A comparison of the two methods shows good agreement in the final converged solution, with the simplex converging to a slightly lower RBM. In addition, the final solution by the simplex method results in a much "tighter" constraint value for HM_{LEI}, where it fell precisely on its upper limit. This is a beneficial characteristic of the simplex method where the optimal solution must lie on a constraint vertex. However, with gradient-based methods, such as the MMOFD, the solution depends heavily on optimization parameters such as move limits and starting point. In complex problems there is then no guarantee that the global optimum is reached.

Overall, the simplex method proved to be better suited for the trim optimization problem as it has been formulated. The simplex solutions, when posed to reflect the MMOFD formulations, converged to slightly better solutions and were more precise in their satisfaction of the constraints. However, the benefits of the simplex method become even more dramatic when the restrictions of the MMOFD are removed, as is evident in the antisymmetric maneuvers.

Table 5 Independent and dependent control surfaces

Maneuver	Independent (basis) surface	Dependent surfaces
1	HT	LEI, LEO, TEI, TEO
2	HT	LEI, LEO, TEI, TEO
3	LEO	LEI, TEI, TEO
4	TEO	LEI, LEO, TEI

Table 6 Final weights for each optimization

Optimization case	Weight, lb
AAW sequential	292.271
AAW optimization 1	405.134
AAW optimization 2	355.50
Conventional control	383.04

Sequential AAW Design Process

The sequential AAW design process, as proposed in Fig. 3, was implemented for the ASTROS optimization model discussed earlier. In addition, three other structural optimizations were performed as a basis of comparison to the sequential process. The first of these, identified as AAW optimization 1, is an ASTROS structural optimization with the optimal control-surface deflections for the starting structural design converted to gear ratios. Over the course of the structural optimization, these gear ratios remain fixed, and the deflections of the independent surfaces are constrained so that none of the surfaces exceed their allowable travel limits. The independent surfaces and dependent surfaces for each maneuver are given in Table 5. The HT was selected as the independent surface for maneuvers 1 and 2 because it has historically been the primary control surface for symmetric trim. The LEO surface was selected for maneuver 3 because it is the most effective surface at supersonic conditions, at which point both trailing-edge surfaces experience control reversal. For maneuver 4 the TEO surface is the independent surface because it is the most effective roll control surface at subsonic speeds.

The second comparison case, identified as AAW optimization 2, is a structural optimization where the dependent surfaces are set to their optimized deflections for the starting structural design and remain fixed over the course of the structural optimization. The independent surfaces remain free during the optimization, deflecting to achieve the prescribed maneuver requirements. For example, for maneuver 1 the deflections of the LEI, LEO, TEI, and TEO surfaces remain fixed at their initial optimal values, and the deflections of the horizontal tail and angle of attack remain free to trim the aircraft.

The final comparison case is structural optimization for a conventionally controlled aircraft, which would be reflective of how current fighter aircraft are controlled. In this case only the horizontal tail is used to trim the aircraft for the symmetric maneuvers. For the supersonic antisymmetric maneuver a blending of the TEI surface and horizontal tail (similar to the F-16) is used to achieve the required roll rate, and for the subsonic antisymmetric maneuver the TEO surface is used. In addition, control-surface effectiveness constraints are added to the structural optimization for the antisymmetric maneuvers, as is typically done for modern fighter aircraft that require high roll rates or fast time to bank.

The final optimized weights for the sequential AAW design process and the three comparison cases are shown in Table 6. By examination of the weights alone, one observes the benefit that is achieved by performing trim optimization for each iteration of the structural optimization. AAW optimization 1 employs AAW technology, but because all of the dependent surfaces are geared to the independent surfaces the independent surfaces have very little "freedom" with which to trim the aircraft. As a result, additional stiffness is added to make the independent surfaces more effective, resulting in an even higher weight than a configuration employing conventional control technology. AAW optimization 2 results in a lower weight solution simply because the independent surfaces are not attached to the dependent surfaces and thus have far more freedom with which to trim the aircraft. However, the weight is not nearly as low as

the sequential process, again emphasizing the need to optimize the control-surface deflections for each structural design (i.e., at each optimization iteration).

Tables 7–10 show the control-surface deflections and trim optimization objective for the final structural iteration of each of the four optimization cases. Table 7 contains the final data for the subsonic, pull-up maneuver, where one clearly sees the benefit of using the wing control surfaces to relieve RBM. For all three AAW cases the outboard control surfaces deflect to their largest negative allowable, which for the leading-edge surface is nose down and for the trailing edge surface is tail up. This has the effect of decreasing the effective angle of attack on the outboard section of the wing, shifting aerodynamic load further inboard, and hence reducing RBM. The three AAW optimization cases result in a 25% reduction in RBM over the conventional control approach. Moreover, in the AAW cases the horizontal tail deflects much less than in the conventional control case. This leads to less tail loading, which probably would have contributed to the reduction of the total structural weight if the tail structure were included in the structural optimization.

Figure 6 is a history of the subsonic, pull-up maneuver control-surface deflections after each structural optimization step of the sequential AAW design process, giving an indication of how the control law evolves as the structural design changes. The dashed line on each plot corresponds to the final deflections for AAW optimization 2. It is seen that the deflections significantly change as the structure is optimized, indicating the importance of conducting a concurrent trim and structural optimization.

Table 8 presents the final trim data for the supersonic, push-over maneuver. Here, once again, one observes the dramatic reduction in the magnitude of RBM for the AAW approaches over a conventional approach. In this case the leading-edge surfaces deflect to their largest positive allowables, which is exactly the opposite trend of maneuver 1. This is because maneuver 2 is a push-over maneuver; hence, RBM is naturally negative, and the goal of trim optimization is to increase RBM, which is achieved by maximal upward deflection of the leading-edge surfaces. Although the trailing-edge

Table 7 Final control-surface deflections and trim objective for subsonic pull-up

Variable	Sequential	AAW optimization 1	AAW optimization 2	Conventional
δ_{LEI}	−4.609 deg	−5.990 deg	−6.350 deg	0.000 deg
δ_{LEO}	−30.056 deg	−28.286 deg	−30.000 deg	0.000 deg
δ_{TEI}	−6.446 deg	−3.231 deg	−3.430 deg	0.000 deg
δ_{TEO}	−30.056 deg	−28.286 deg	−30.000 deg	0.000 deg
δ_{HT}	0.790 deg	1.430 deg	1.383 deg	−4.799 deg
α	11.751 deg	11.784 deg	11.699 deg	10.072 deg
RBM, lb-in.	4,701,820.0	4,614,680.0	4,629,120.0	6,238,330.0

Table 8 Final control-surface deflections and trim objective for supersonic push-over

Variable	Sequential	AAW optimization 1	AAW optimization 2	Conventional
δ_{LEI}	4.998 deg	4.499 deg	5.000 deg	0.000 deg
δ_{LEO}	4.998 deg	4.499 deg	5.000 deg	0.000 deg
δ_{TEI}	−29.290 deg	−26.005 deg	−28.900 deg	0.000 deg
δ_{TEO}	15.480 deg	13.537 deg	15.040 deg	0.000 deg
δ_{HT}	2.695 deg	2.603 deg	2.660 deg	2.217 deg
α	−2.213 deg	−2.152 deg	−2.210 deg	−1.600 deg
RBM, lb-in.	−1,328,030.0	−1,406,360.0	−1,324,950.0	−2,111,000.0

Table 9 Final control-surface deflections and trim objective for supersonic roll

Variable	Sequential	AAW optimization 1	AAW optimization 2	Conventional
δ_{LEI}	0.705 deg	0.714 deg	0.715 deg	0.000 deg
δ_{LEO}	4.732 deg	4.995 deg	5.000 deg	0.000 deg
δ_{TEI}	0.033 deg	0.115 deg	0.115 deg	16.503 deg
δ_{TEO}	1.093 deg	11.533 deg	11.547 deg	0.000 deg
HM_{total}, lb-in.	48,991.7	82,156.0	80,488.1	115,045.1

Table 10 Final control-surface deflections and trim objective for subsonic roll

Variable	Sequential	AAW optimization 1	AAW optimization 2	Conventional
δ_{LEI}	3.165 deg	2.774 deg	2.774 deg	0.000 deg
δ_{LEO}	5.016 deg	4.989 deg	5.000 deg	0.000 deg
δ_{TEI}	−2.385 deg	−1.527 deg	−1.530 deg	0.000 deg
δ_{TEO}	15.291 deg	10.753 deg	12.064 deg	14.797 deg
HM_{total}, lb-in.	39,330.9	28,369.3	32,859.5	90,971.1

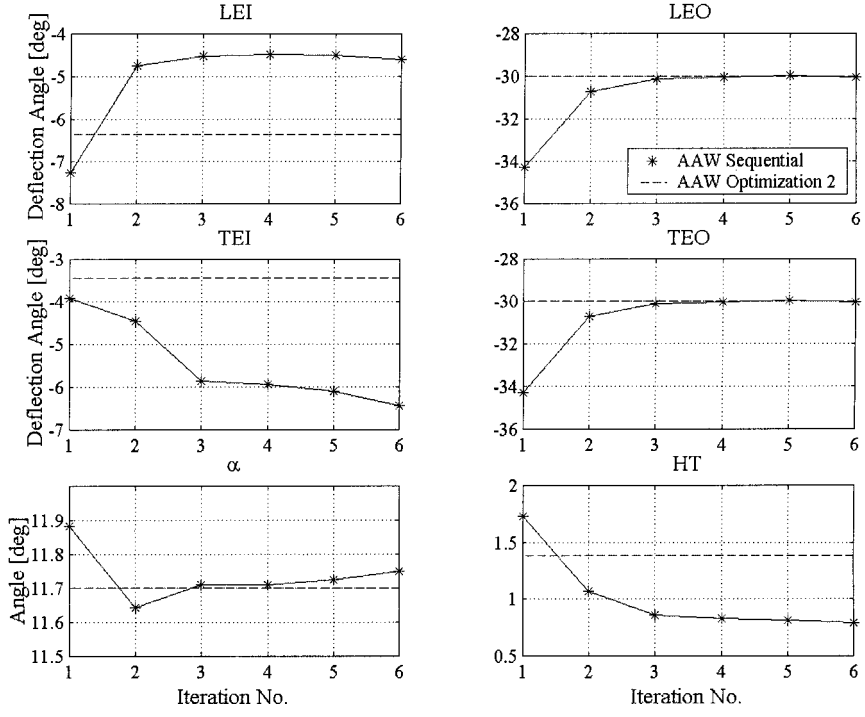

Fig. 6 Control-surface deflection history (maneuver 1).

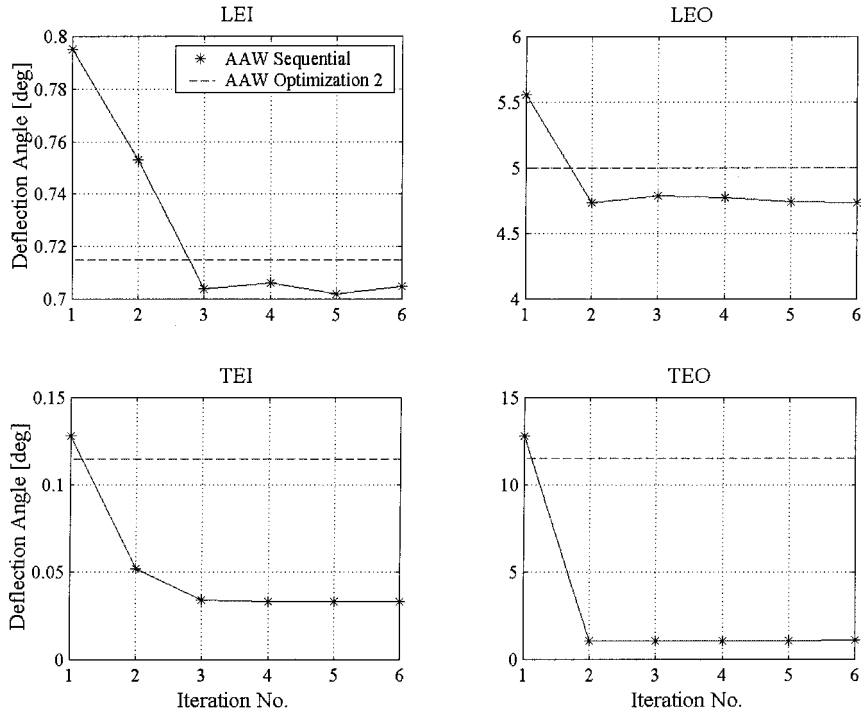

Fig. 7 Control-surface deflection history (maneuver 3).

surfaces deflect to rather large values, their ineffectiveness at supersonic speeds results in them having little effect on the RBM, and thus they are used primarily to meet the hinge moment constraints.

Table 9 presents the final data for the supersonic, rolling maneuver, showing the same trends that were observed for the previous maneuvers. Examination of the final control-surface deflections for each of the three AAW optimization cases reveals that as the structure is modified the trailing-edge surfaces are used less and less to achieve the required roll rate. This is made apparent by the lower deflection of the trailing-edge surfaces for the sequential approach compared to the other AAW optimization cases. In AAW optimization 1 and 2 the TEO surface is used rather extensively, as these cases correspond to the optimal control laws for the starting structural design, but as is evident by the higher total hinge moment, they are not optimal for the final structural design.

This point is also reinforced in Fig. 7, which is a plot of the control-surface deflections for each iteration of the sequential AAW design process for this maneuver. The dashed line on each plot refers to the final control-surface deflection of AAW optimization 2. One sees that after the first iteration usage of the TEO surface drops off dramatically. This is because from iteration 1 to iteration 2 the TEO control surface begins to reverse, and hence the trim optimization deemphasizes this surface in favor of the leading-edge surfaces. However, both AAW optimization 1 and 2 are forced to use this surface as they employ the starting optimal control law and, as a result, pay a rather significant penalty in hinge moment because of its heavy use.

Finally, Table 10 contains the final trim data for the subsonic rolling maneuver. In contrast to the supersonic rolling maneuver, the TEO surface is used rather heavily. This is because at the subsonic Mach number this surface is still effective. Although the total hinge moment by the sequential process is higher than either of the other two AAW optimization cases, the structure is much lighter and more flexible. Thus, the loads acting on this structure produce higher hinge moments. Also, note the significant reduction in total hinge moment when the leading-edge surfaces are employed as seen by comparing the AAW cases to the conventional control design.

Conclusion

Trim optimization for AAW technology has been performed using the simplex method and compared against previous trim optimization results that were generated using a gradient-based MMOFD optimization algorithm. The results of this comparison revealed that the simplex method converged to comparable and slightly better solutions when posed in the same manner as trim optimization by the MMOFD. However, when the nonphysical constraints that were applied to trim optimization by the MMOFD were removed, the simplex method produced significantly better results as seen by a 73% reduction in total hinge moments for the subsonic roll and a 61% reduction in total hinge moments for the supersonic roll. In general, the simplex method was better suited for the type of trim optimization problems being solved, whose constraints and objectives were linear functions of the design variables.

Trim optimization by the simplex method was then integrated into the sequential AAW design process, in which structural optimization and trim optimization are repeated in an iterative fashion. Comparison of final results of the sequential process with a conventional control case demonstrated a nearly 24% reduction in weight with the use of AAW technology. Comparison of the sequential AAW design to designs based on fixed control laws demonstrated the importance of optimizing the control law following each structural optimization. This is evidenced by the significant reductions in weight and different final control-surface deflections of the sequential AAW design process over AAW optimization 1 and 2. The current effort of the authors is focused on the direct integration of the trim optimization into the ASTROS structural optimization scheme, in order to accommodate the concurrent trim-structural optimization.

Acknowledgments

The authors extend thanks to Mordechay Karpel and Boris Moulin of Technion—Israel Institute of Technology for their technical advice and assistance on ASTROS. In addition, the authors thank Michael Love of Lockheed Martin Tactical Aircraft Systems for his involvement in trim optimization by the modified method of feasible directions.

References

[1]Miller, G. D., "Active Flexible Wing (AFW) Technology," Air Force Wright Aeronautical Lab., TR-87-3096, Dayton, OH, Feb. 1988.

[2]Perry, B., III, Cole, S. R., and Miller, G. D., "A Summary of an AFW Program," *Journal of Aircraft*, Vol. 32, No. 1, 1995, pp. 10–15.

[3]Pendleton, E. W., Bessette, D., Field, P. B., Miller, G. D., and Griffin, K. E., "Active Aeroelastic Wing Flight Research Program: Technical Program and Model Analytical Development," *Journal of Aircraft*, Vol. 37, No. 4, 2000, pp. 554–561.

[4]Flick, P. M., Love, M. H., and Zink, P. S., "The Impact of Active Aeroelastic Wing Technology on Conceptual Aircraft Design," *Proceedings of the RTO Applied Vehicle Technology Specialists' Meeting on* "Structural Aspects of Flexible Aircraft Control," RTO MP-36, NATO Research and Technology Agency, Ottawa, Canada, Oct. 1999.

[5]Volk, J., and Ausman, J., "Integration of a Generic Flight Control System into ASTROS," AIAA Paper 96-1335, April 1996.

[6]Neill, D. J., Johnson, E. H., and Canfield, R., "ASTROS—A Multidisciplinary Automated Design Tool," *Journal of Aircraft*, Vol. 27, No. 12, 1990, pp. 1021–1027.

[7]Ausman, J., and Volk, J., "Integration of Control Surface Load Limiting into ASTROS," AIAA Paper 97-1115, April 1997.

[8]Forster, E., Kolonay, R., Venkayya, V., and Eastep, F., "Optimization of a Generic Fighter Wing Incorporating Active Aeroelastic Wing Technology," AIAA Paper 96-4010, Sept. 1996.

[9]Anderson, G., Forster, E., Kolonay, R., and Eastep, F., "Multiple Control Surface Utilization in Active Aeroelastic Wing Technology," *Journal of Aircraft*, Vol. 34, No. 4, 1997, pp. 552–557.

[10]Miller, G. D., "An Active Flexible Wing Multi-Disciplinary Design Optimization Method," AIAA Paper 94-4412, Sept. 1994.

[11]Zillmer, S., "Integrated Multidisciplinary Optimization for Active Aeroelastic Wing Design," Air Force Wright Aeronautical Lab., WL-TR-97-3087, Dayton, OH, Aug. 1997.

[12]Rodden, W. P., and Johnson, E. H., "MSC/NASTRAN Version 68 Aeroelastic Analysis User's Guide," The Macneal-Schwendler Corp., Pasadena, CA, 1994.

[13]Dobbs, S. K., Schwanz, R. C., and Abdi, F., "Automated Structural Analysis Process at Rockwell," *Proceedings of the 82nd Meeting of the AGARD Structures and Materials Panel on* "Integrated Airframe Design Technology," AGARD Rept. 814, North Atlantic Treaty Orginization, Sesimbra, Portugal, May 1996.

[14]Love, M. H., Barker, D. K., Egle, D. D., Neill, D. J., and Kolonay, R. M., "Enhanced Maneuver Airloads Simulation for the Automated Structural Optimization System—ASTROS," AIAA Paper 97-1116, April 1997.

[15]Vanderplaats, G. N., "An Efficient Feasible Directions Algorithm for Design Synthesis," *AIAA Journal*, Vol. 22, No. 11, 1984, pp. 1633–1640.

[16]Zink, P. S., Mavris, D. N., Flick, P. M., and Love, M. H., "Development of Wing Structural Weight Equation for Active Aeroelastic Wing Technology," *Journal of Aerospace*, Sec. 1, Vol. 108, 1999, pp. 1421–1431.

[17]Chvátal, V., *Linear Programming*, W. H. Freeman and Co., New York, 1983, p. 222.

[18]Vanderplaats, G. N., *Numerical Optimization Techniques for Engineering Design: With Applications*, McGraw–Hill, New York, 1984, pp. 110–116.

[19]Dantzig, G. B., Orden, A., and Wolfe, P., "The Generalized Simplex Method for Minimizing a Linear Form Under Linear Inequality Restraints," *Pacific Journal of Mathematics*, Vol. 5, No. 1, 1955, pp. 183–195.

[20]Johnson, E. H., and Venkayya, V. B., "Automated Structural Optimization System (ASTROS), Vol. 1—Theoretical Manual," Air Force Wright Aeronautical Lab., AFWAL-TR-88-3028, Dayton, OH, Dec. 1988.

[21]Rodden, W. P., and Love, J. R., "Equations of Motion of Quasisteady Flight Vehicle Utilizing Restrained Static Aeroelastic Characteristics," *Journal of Aircraft*, Vol. 22, No. 9, 1995, pp. 802–809.

[22]"Optimization Toolbox for Use with MATLAB—User's Guide, Version 2," MathWorks, Inc., Natick, MA, 1999.

[23]Karpel, M., Moulin, B., and Love, M. H., "Modal-Based Structural Optimization with Static Aeroelastic and Stress Constraints," *Journal of Aircraft*, Vol. 34, No. 3, 1997, pp. 433–440.

[24]Zink, P. S., Mavris, D. N., Love, M. H., and Karpel, M., "Robust Design for Aeroelastically Tailored/Active Aeroelastic Wing," AIAA Paper 98-4781, Sept. 1998.

[25]Carmichael, R. L., Castellano, C. R., and Chen, C. F., "The Use of Finite Element Methods for Predicting the Aerodynamics of Wing-Body Combinations," NASA SP-228, Oct. 1969.

[26]Barker, D. K., and Love, M. H., "An ASTROS Application with Path Dependent Results," AIAA Paper 96-4139, Sept. 1996.